

Nonlinear Precoders for Massive MIMO Systems with General Constraints

(Invited Paper)

Ali Bereyhi, Mohammad Ali Sedaghat, Saba Asaad, Ralf R. Müller

Institute for Digital Communications (IDC), Friedrich-Alexander Universität Erlangen-Nürnberg (FAU)
ali.bereyhi@fau.de, mohammad.sedaghat@fau.de, saba.asaad@fau.de, ralf.r.mueller@fau.de

Abstract—We introduce a class of nonlinear least square error precoders with a general penalty function for multiuser massive MIMO systems. The generality of the penalty function allows us to consider several hardware limitations including transmitters with a predefined constellation and restricted number of active antennas. The large-system performance is then investigated via the replica method under the assumption of replica symmetry. It is shown that the least square precoders exhibit the “marginal decoupling property” meaning that the marginal distributions of all precoded symbols converge to a deterministic distribution. As a result, the asymptotic performance of the precoders is described by an equivalent single-user system. To address some applications of the results, we further study the asymptotic performance of the precoders when both the peak-to-average power ratio and number of active transmit antennas are constrained. Our numerical investigations show that for a desired distortion at the receiver side, proposed forms of the least square precoders need to employ around 35% fewer number of active antennas compared to cases with random transmit antenna selection.

Index Terms—Nonlinear least square error precoders, limited peak-to-average power ratio, transmit antenna selection, marginal decoupling property, replica method.

I. INTRODUCTION

The concept of massive Multiple-Input Multiple-Output (MIMO) systems has been considered to be a key solution to vast demands for higher performance gains such as spectral efficiency, rate reliability, and energy efficiency [1]. These benefits are obtained along with hardware challenges arising due to the tremendous number of antennas. Some of these issues, such as having a large antenna array within a relatively small physical platform, are effectively addressed by utilizing the millimeter wave spectrum [2]; however, some other issues such as overall Radio Frequency (RF) cost and energy efficiency are still remained as bottlenecks and need to be overcome by effective design of system modules.

In this paper, our concentration is on the downlink scenario. The module which plays a key role in this case is the precoder which maps the data signal to a precoded signal in order to compensate the distortion caused by the channel. This leads to a receive signal with low distortion, and therefore, the processing load at the user side reduces significantly. Primary approaches for precoding are the linear schemes which have lower computational complexity, e.g., Match Filtering (MF)

and Regularized Zero Forcing (RZF). More advanced approaches such as Tomlinson-Harashima [3] and vector precoding [4], however, achieve a better performance at the expense of more complexity. Although these schemes take into account the computational complexity of the precoding algorithms, they do not consider limitations imposed to the system by hardware restrictions. As an example, the aforementioned precoders consider the whole complex plane as the set of possible transmit constellation points; the assumption which in practice does not hold, due to the limited Peak-to-Average Power Ratio (PAPR) of power amplifiers. The authors in [5] tried to address this drawback partially by proposing the nonlinear “per-antenna constant envelope precoding” in which the precoder maps the data signal such that the precoded signal has a constant amplitude. In [6], a class of nonlinear Least Square Error (LSE) precoders was introduced where the precoder minimizes the distortion at the receiver side over a general transmission support considering a constraint on the transmit power. The generality of the transmission support enabled the authors in [6] to investigate more general scenarios, such as transmitters with restricted PAPR, and discrete transmit constellations. In this paper, we study the nonlinear LSE precoders considering a general penalty function which enables us to investigate various limitations on the transmitter including constraints on the limited number of RF-chains.

Transmit Antenna Selection

One of the crucial bottlenecks in massive MIMO systems is the large overall RF cost. In the downlink scenario, this is mainly caused by the vast number of RF chains connected to transmit antennas. In this case, Transmit Antenna Selection (TAS) can significantly reduce hardware costs without significant performance loss [7]. Regarding massive MIMO systems, the optimal TAS becomes computationally unfeasible, due to exponentially increasing number of searches. Alternatively, suboptimal greedy algorithms with polynomial order of complexity can be employed [8], [9]. From the analytical point of view, the study of TAS algorithms in large-system limits faces more difficulties, and has been addressed in the literature only for some special selection algorithms invoking tools from order statistics; see [10], [11] and references therein.

The limited RF cost of the system can be addressed directly at the precoder instead of employing TAS algorithms. In fact, by constraining the precoded signal to have a certain number

This work was supported by the German Research Foundation, Deutsche Forschungsgemeinschaft (DFG), under Grant No. MU 3735/2-1.

of zero entries, the precoder selects a subset of transmit antennas while it maps the data signal to the constellation points.

Contributions

In this paper, a large class of nonlinear LSE precoders is introduced with a general penalty function which is able to address several transmit limitations. In the large-system limit, we evaluate the performance of the precoder in terms of an equivalent single-user system. Using this asymptotic result, we show that the precoder exhibits an ‘‘asymptotic marginal decoupling property’’. This means that the output symbols of the precoder have identical marginal distributions which are equal to the marginal output distribution of the equivalent single-user system. The asymptotic results of this paper are derived via the replica method from statistical mechanics considering Replica Symmetry (RS). An introduction to the replica method is given through the asymptotic analyses, in the appendix.

Notation

We represent scalars, vectors and matrices with non-bold, bold lower case and bold upper case letters, respectively. A $k \times k$ identity matrix is shown by \mathbf{I}_k , and \mathbf{H}^H indicates the Hermitian of the matrix \mathbf{H} . The set of real and integer numbers are denoted by \mathbb{R} and \mathbb{Z} , and their corresponding non-negative subsets are shown by superscript $+$; moreover, \mathbb{C} represents the complex plane. $\|\mathbf{x}\|$ denotes the Euclidean norm of the vector \mathbf{x} , and $\|\mathbf{x}\|_0$ represents the zero-norm defined as the number of nonzero entries. For a random variable x , p_x represents either the probability mass or probability density function. Moreover, the expectation operator is denoted by \mathbb{E} . For sake of compactness, the set of integers $\{1, \dots, n\}$ is abbreviated as $[1 : n]$. Whenever needed, we consider the entries of \mathbf{x} to be discrete random variables, namely the support \mathbb{X} to be discrete. Our results, however, are in full generality and hold also for continuous distributions as well.

II. PROBLEM FORMULATION

The nonlinear LSE precoding scheme with general penalty, employed in a multiuser MIMO system, is defined as

$$\mathbf{x}(\mathbf{s}, \mathbf{H}) = \arg \min_{\mathbf{v} \in \mathbb{X}^n} \|\mathbf{H}\mathbf{v} - \mathbf{s}\|^2 + u(\mathbf{v}) \quad (1)$$

where $\mathbf{H} \in \mathbb{C}^{k \times n}$ and $\mathbf{s} \in \mathbb{C}^{k \times 1}$ denote the channel matrix and data vector, and $u(\cdot)$ is a function which decouples, i.e.,

$$u(\mathbf{v}) = \sum_{j=1}^n u(v_j). \quad (2)$$

We assume \mathbf{H} to be a random matrix with decomposition

$$\mathbf{H}^H \mathbf{H} = \mathbf{U} \mathbf{D} \mathbf{U}^H \quad (3)$$

where $\mathbf{U}_{n \times n}$ is a Haar distributed unitary matrix, and $\mathbf{D}_{n \times n}$ is a diagonal matrix with asymptotic eigenvalue distribution p_D . The ensemble of \mathbf{H} encloses a large class of MIMO channel models including the well-known independent and identically distributed (i.i.d.) Rayleigh fading model. $\mathbf{s}_{k \times 1}$ is independent of \mathbf{H} and considered to have i.i.d. zero-mean complex Gaussian entries with variance λ_s , i.e., $\mathbf{s} \sim \mathcal{CN}(\mathbf{0}, \lambda_s \mathbf{I}_k)$. We let the

dimensions of \mathbf{H} grow large assuming the load factor, defined as $\alpha := k/n$, is asymptotically constant in both k and n . For sake of brevity, we drop the dependence of \mathbf{x} on \mathbf{s} and \mathbf{H} .

By setting the penalty function $u(\cdot)$ and the support \mathbb{X} to be of some given forms, the precoder in (1) reduces to several specific precoders. As examples, let $u(\mathbf{v}) = \lambda \|\mathbf{v}\|^2$; then,

- (a) by setting $\mathbb{X} = \mathbb{C}$, the precoder reduces to the RZF precoder [4] which reads

$$\mathbf{x} = \mathbf{H}^H (\mathbf{H} \mathbf{H}^H + \lambda \mathbf{I}_k)^{-1} \mathbf{s}. \quad (4)$$

- (b) for \mathbb{X} being a circle in the complex plane, the precoder reduces to the constant envelope precoder considered in [5].
- (c) when \mathbb{X} is set to be a general subset of \mathbb{C} , the precoder reduces to the nonlinear LSE precoder introduced in [6].

The precoder considered in (1) addresses the above precoding schemes as well as some other techniques which consider different constraints. To study the large-system properties of the precoder, we define the following asymptotic parameters.

Definition 1 (Asymptotic Marginal): Consider the precoded vector $\mathbf{x}_{n \times 1}$, and function $f(\cdot)$ defined as

$$f(\cdot) : \mathbb{X} \mapsto \mathbb{R}. \quad (5)$$

Define the marginal of $f(\mathbf{x})$ over $\mathbb{W}(n) \subseteq [1 : n]$ as

$$\mathbb{M}_f^{\mathbb{W}}(\mathbf{x}; n) := \frac{1}{|\mathbb{W}(n)|} \sum_{w \in \mathbb{W}(n)} \mathbb{E} f(x_w) \quad (6)$$

The asymptotic marginal of $f(\mathbf{x})$ is then defined to be the large limit of $\mathbb{M}_f^{\mathbb{W}}(\mathbf{x}; n)$, i.e., $\mathbb{M}_f^{\mathbb{W}}(\mathbf{x}) := \lim_{n \uparrow \infty} \mathbb{M}_f^{\mathbb{W}}(\mathbf{x}; n)$.

Definition 2 (Asymptotic Distortion): For the precoder defined in (1), the asymptotic input-output distortion is defined as

$$\mathbb{D} := \lim_{k \uparrow \infty} \frac{1}{k} \mathbb{E} \|\mathbf{H}\mathbf{x} - \mathbf{s}\|^2. \quad (7)$$

where \mathbf{x} is the precoded vector given in (1).

The asymptotic marginal describes the statistical properties of \mathbf{x} in the large limit. Moreover, Definition 2 determines the distortion between the noise-free version of the channel output, i.e., $\mathbf{H}\mathbf{x}$, and the data vector. Our goal is to determine the asymptotic distortion as well as the asymptotic marginal of $f(\mathbf{x})$ for a given function $f(\cdot)$. To overcome this task, we invoke the replica method. The results then let us investigate several configurations of the precoder which address different criteria such as power constraint, PAPR control and TAS.

III. MAIN RESULTS

Our main result gives closed-form expression for the asymptotic distortion and marginal of $f(\mathbf{x})$ considering a large class of random channel matrices. Before stating the results, let us define the R-transform of a given probability distribution.

Definition 3 (R-transform): For the random variable t with distribution p_t , the Stieltjes transform over the upper complex half plane is given by $G_t(s) = \mathbb{E}(t - s)^{-1}$. Let $G_t^{-1}(\cdot)$ denote the inverse with respect to (w.r.t.) composition. Then,

the R-transform of the distribution p_t is defined as $R_t(\omega) = G_t^{-1}(-\omega) - \omega^{-1}$ such that $\lim_{\omega \downarrow 0} R_t(\omega) = E t$.

For the random matrix \mathbf{H} specified in Section II, the R-transform of the Gramian $\mathbf{H}^H \mathbf{H}$ is defined w.r.t. the asymptotic eigenvalue distribution $p_{\mathbf{D}}$, and denoted by $R_{\mathbf{D}}(\cdot)$. Proposition 1 gives the asymptotics of the precoder in terms of $R_{\mathbf{D}}(\cdot)$.

Proposition 1 (RS Ansatz): Consider the nonlinear LSE precoder defined in Section II, and assume a set of assumptions, including replica continuity and RS, holds. Let s^{rs} be a zero-mean complex Gaussian random variable with variance λ^{rs} which for some χ and ρ reads as follows

$$\lambda^{rs} = [R_{\mathbf{D}}(-\chi)]^{-2} \frac{\partial}{\partial \chi} [(\lambda_s \chi - \rho) R_{\mathbf{D}}(-\chi)]. \quad (8)$$

Moreover, define the random variable x to be

$$x = \arg \min_v |v - s^{rs}|^2 + [R_{\mathbf{D}}(-\chi)]^{-1} u(v). \quad (9)$$

with $v \in \mathbb{X}$. Then, the asymptotic marginal of $f(x)$ is given by

$$M_f^{\mathbb{W}}(x) = E f(x), \quad (10)$$

and the asymptotic distortion is determined as

$$D = \lambda_s + \alpha^{-1} \frac{\partial}{\partial \chi} [(\rho - \lambda_s \chi) \chi R_{\mathbf{D}}(-\chi)] \quad (11)$$

when ρ is set to be the average transmit power of the precoder determined as $\rho = E |x|^2$ and χ satisfies the fixed point equation

$$\chi R_{\mathbf{D}}(-\chi) = \frac{1}{\lambda^{rs}} E \text{Re} \{x^* s^{rs}\}. \quad (12)$$

Proof: The proof is briefly sketched in the appendix, and the detailed derivations are left for the extended version of the manuscript.

Proposition 1 determines the asymptotic distortion by solving a set of fixed point equations. It implies moreover that under the set of supposed assumptions, i.e., replica continuity and RS

- (a) the asymptotic marginal of $f(x)$ does not depend on the index set $\mathbb{W}(n)$.
- (b) the asymptotic marginal of $f(x)$ is equal to the expected marginal of an equivalent single-user nonlinear LSE precoder which maps s^{rs} to x via (9).

These findings lead us to conclude this property of the precoder that the output symbols marginally decouple into the outputs of similar single-user nonlinear LSE precoders. This property is referred to as the ‘‘RS marginal decoupling property’’ and is deduced directly from Proposition 1.

A. RS Marginal Decoupling Property

For different classes of estimators, the decoupling property has been investigated in the literature, e.g. [12]–[14]. The main idea of this property is that for a given estimator, the joint distribution of almost any pair of input-output symbols converges to a fixed distribution which is constant in terms of the symbols’ index. We show that a marginal version of the decoupling property holds for nonlinear LSE precoders as well.

To illustrate the property, let us denote the marginal distribution of the j th symbol of $\mathbf{x}_{n \times 1}$, i.e., x_j for $j \in [1 : n]$, by $p_x^{j(n)}$ where the superscript n indicates the dependency on the length of \mathbf{x} . Moreover, we define p_x^j to be the asymptotic limit of $p_x^{j(n)}$ meaning that for $t \in \mathbb{X}$

$$p_x^j(t) := \lim_{n \uparrow \infty} p_x^{j(n)}(t). \quad (13)$$

The RS marginal decoupling property states that, under RS, p_x^j is constant in j for any $j \in [1 : n]$. Therefore, one can consider the precoded symbols to be outputs of copies of a single-user nonlinear LSE precoder consistent with (9). More precisely, considering the marginal distributions, the entries of the precoded vector \mathbf{x} are identically distributed with the distribution of the random variable x defined in (9). We call this random variable ‘‘decoupled precoded symbol’’ and denote its marginal distribution with p_x .

Proposition 2 (RS Marginal Decoupling Property): Let the nonlinear LSE precoder satisfy the constraints given in Section II. Then, under some assumptions including the replica continuity and RS, the symbol x_j , for any $j \in [1 : n]$, converges in distribution to the random variable x given in (9).

Proof: The proof directly follows from Proposition 1. Let the function $f(\cdot)$ be

$$f(x) = \delta(x - t) \quad (14)$$

and consider the index set $\mathbb{J}(n) = [j : j + \zeta n]$. Substituting in Definition 1, the marginal of $f(x)$ reads

$$M_f^{\mathbb{J}}(\mathbf{x}; n) = \frac{1}{1 + \zeta n} \sum_{w=j}^{j+\zeta n} E \delta(x_w - t) \quad (15a)$$

$$= \frac{1}{1 + \zeta n} \sum_{w=j}^{j+\zeta n} p_x^{w(n)}(t). \quad (15b)$$

As $\zeta \downarrow 0$, $M_f^{\mathbb{J}}(\mathbf{x}; n)$ converges to $p_x^{j(n)}(t)$, and thus,

$$p_x^j(t) = \lim_{n \uparrow \infty} \lim_{\zeta \downarrow 0} M_f^{\mathbb{J}}(\mathbf{x}; n). \quad (16)$$

As Proposition 1 indicates, the asymptotic marginal of $f(x)$ does not depend on the index set $\mathbb{J}(n)$. This concludes that for any ζ in vicinity of zero, $\lim_{n \uparrow \infty} M_f^{\mathbb{W}}(\mathbf{x}; n)$ converges to a same value. Consequently, the limit w.r.t. ζ in (16) can be dropped, and one can write

$$p_x^j(t) = M_f^{\mathbb{J}}(\mathbf{x}). \quad (17)$$

(17) indicates that $p_x^j(t)$ is constant in j . By substituting (14) in Proposition 1, it is straightforwardly shown that $M_f^{\mathbb{J}}(\mathbf{x})$ is equal to the distribution of x at the point t , i.e., $p_x(t)$, which concludes the proof.

Remark 1: In the proof of Proposition 2, the convergence of $M_f^{\mathbb{J}}(\mathbf{x}; n)$ might be questioned, due to the singularity of the function $f(\cdot)$ defined in (14). To avoid this issue, one can take an alternative approach by defining $f(x)$ to be non-negative integer powers of x . In this case, the marginal asymptotic of

$f(\mathbf{x})$ determines the moments of x_j . Using results from the classical moment problem [15], it is then trivial to conclude the decoupling property. More details are found in [12], [14].

Proposition 2 justifies intuitive findings from Proposition 1. In fact, one can consider (9) as a single-user system whose expected performance describes the asymptotic average performance of the nonlinear LSE precoder.

IV. APPLICATIONS OF THE RESULTS

The results given in Section III apply to various

- (a) particular precoders as special cases,
- (b) models of MIMO fading channels including the well-known i.i.d. Rayleigh fading model,
- (c) constraints on MIMO transmitters, such as peak and average power constraints, and TAS.

In this section, we employ the results to study the asymptotics of some particular precoders. Through out the examples, we consider the channel matrix \mathbf{H} to be an i.i.d. fading channel whose entries are i.i.d. zero-mean random variables with variance n^{-1} . In this case, $p_{\mathbf{D}}$ follows Marcenko-Pastur law [16], and therefore, the R-transform reads

$$R_{\mathbf{D}}(\omega) = \frac{\alpha}{1 - \omega}. \quad (18)$$

A. Average Power Constraint and TAS

The initial form of the nonlinear LSE precoder, introduced in [6], considers the penalty function $u(\cdot)$ to be proportional to the Euclidean norm, i.e., $u(\mathbf{v}) = \lambda \|\mathbf{v}\|^2$. This penalty function controls the average power of the precoded vector, i.e., $n^{-1} \mathbb{E} \|\mathbf{x}\|^2$, and thus, can satisfy different constraints on the average power by correspondingly setting λ . Considering the precoder defined in Section II, the generality of the utility function lets the precoder take into account the TAS in addition to the average power constraint. In order to address both the constraints at the precoder, we consider $u(\cdot)$ to be

$$u(\mathbf{v}) = \lambda \|\mathbf{v}\|^2 + \lambda_0 \|\mathbf{v}\|_0. \quad (19)$$

The penalty function in (19) imposes constraints on both the average power and number of active antennas by different values of λ and λ_0 considering a same discussion as given at the beginning of this section. As the first step for investigating the precoder consistent with (19), we consider the case in which the precoded symbols are taken from the complex plane, i.e., $\mathbb{X} = \mathbb{C}$. In this case, the decoupled precoded symbol reads

$$\mathbf{x} = \begin{cases} \frac{s^{rs}}{1 + \kappa\lambda} & |s^{rs}| \geq \tau \\ 0 & |s^{rs}| < \tau \end{cases} \quad (20)$$

where $s^{rs} \sim \mathcal{CN}(0, \lambda^{rs})$ and $\tau := \sqrt{\kappa\lambda_0(1 + \kappa\lambda)}$. Here, the variance λ^{rs} , is given by $\lambda^{rs} = \alpha^{-1}(\lambda_s + p)$ where p denotes the average transmit power of the precoder, or alternatively, the expected power of the decoupled precoded symbol, i.e.,

$$p = \lim_{n \uparrow \infty} \frac{1}{n} \|\mathbf{x}\|^2 = \mathbb{E} |x|^2 = \frac{\lambda^{rs} + \tau^2}{(1 + \kappa\lambda)^2} e^{-\frac{\tau^2}{\lambda^{rs}}}. \quad (21)$$

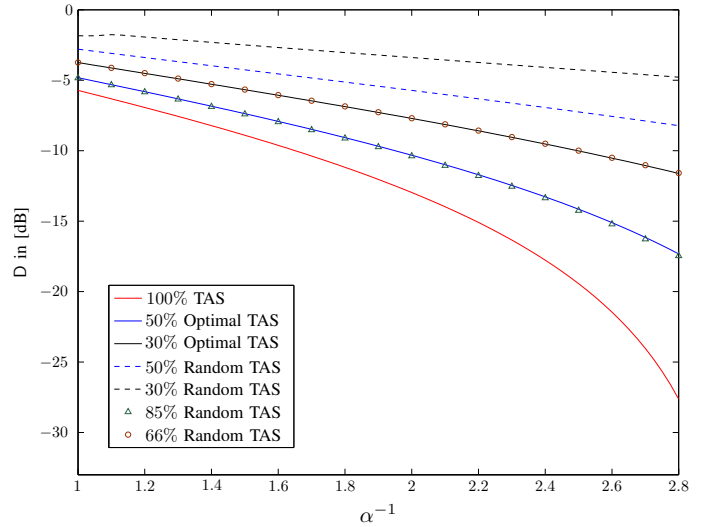


Fig. 1: RS predicted asymptotic distortion as a function of inverse load factor for $p = 0.5$ considering TAS constraints $\eta = 0.5$ and $\eta = 0.3$. The nonlinear LSE precoder with penalty function (19) results in a same distortion as the RZF with random TAS by using about $0.35n$ fewer number of transmit antennas.

Moreover, the scalar κ is defined as $\kappa := \alpha^{-1}(1 + \chi)$ where the non-negative scalar χ satisfies

$$\lambda^{rs} \chi = \kappa p + \kappa^2 \lambda p. \quad (22)$$

Considering (20), the decoupled precoded symbol is obtained by hard thresholding the complex Gaussian symbol s_{rs} in which the threshold τ depends on the control factor λ_0 . By setting $\lambda_0 = 0$, the threshold becomes zero as well, and thus, the decoupled precoded symbol reduces to a complex Gaussian random variable describing the marginal distribution of RZF precoder's output symbols. To investigate the constraint on the number of active antennas, we determine the asymptotic fraction of active antennas η . Using Proposition 1, η reads

$$\eta = \lim_{n \uparrow \infty} \frac{1}{n} \|\mathbf{x}\|_0 = \mathbb{E} \mathbf{1}\{x \neq 0\} = e^{-\frac{\tau^2}{\lambda^{rs}}}. \quad (23)$$

where $\mathbf{1}\{\cdot\}$ denotes the indicator function. Considering given constraints on p and η , one can determine the corresponding control factors λ and λ_0 , as well as the scalar χ , by solving the set of fixed point equations in (21), (22) and (23). The asymptotic distortion is then determined from Proposition 1 as

$$D = \frac{\lambda_s + p}{(1 + \chi)^2}. \quad (24)$$

Fig. 1 shows the asymptotic distortion in terms of the inverse load factor, i.e., α^{-1} , considering various constraints on the fraction of active antennas when the control factor λ is selected such that $p = 0.5$. Moreover, the source variance is set to be $\lambda_s = 1$. As the figure illustrates, the RS ansatz predicts that the precoder with a given constraint on η significantly outperforms the RZF precoder with random TAS¹. To quantify

¹In fact, in this case, the precoder selects a subset of transmit antennas randomly and precodes \mathbf{s} using the penalty function $u(\mathbf{v}) = \lambda \|\mathbf{v}\|^2$.

the improvement, we have plotted the asymptotic distortion for the RZF precoder with random TAS considering several values of η . The numerical investigations depict that for a given asymptotic distortion, the nonlinear LSE precoder with penalty function (19) requires around $0.35n$ fewer number of active antennas compared to a RZF precoder with random TAS.

B. Peak Power Constraint and TAS

Active transmit antennas, in practice, are equipped with power amplifiers whose peak powers are restricted. Therefore, assuming the whole complex plane as the set of possible constellation points of the precoder's output is an inaccurate model for many systems. The inaccuracy is more pivotal when the transmit signal is desired to have a relatively small PAPR. This issue can be addressed by enforcing the precoder to take transmit symbols from

$$\mathbb{X} = \left\{ r e^{j\theta} : 0 \leq \theta \leq 2\pi \wedge 0 \leq r \leq \sqrt{P} \right\}. \quad (25)$$

In this case, the output symbols are restricted to lie inside a circle with radius \sqrt{P} , and thus, the transmit per-antenna peak power is upper bounded by P . By considering a penalty function as in (19), we can further impose a TAS constraint on the precoder. Consequently, the decoupled precoded symbol is given by two steps of hard thresholding as

$$\mathbf{x} = \begin{cases} \frac{s^{rs}}{|s^{rs}|} \sqrt{P} & \hat{\tau} \leq |s^{rs}| \\ 0 & \tilde{\tau} \leq |s^{rs}| < \hat{\tau} \\ \frac{s^{rs}}{1 + \kappa\lambda} & \tau \leq |s^{rs}| \leq \tilde{\tau} \\ 0 & 0 \leq |s^{rs}| < \tau \end{cases} \quad (26)$$

where $s^{rs} \sim \mathcal{CN}(0, \lambda^{rs})$ and the thresholds τ , $\tilde{\tau}$, and $\hat{\tau}$ read

$$\tau := \sqrt{\kappa\lambda_0(1 + \kappa\lambda)} \quad (27a)$$

$$\tilde{\tau} := (1 + \kappa\lambda)\sqrt{P} \quad (27b)$$

$$\hat{\tau} := \max \left\{ (1 + \kappa\lambda)\sqrt{P}, \frac{1 + \kappa\lambda}{2}\sqrt{P} + \frac{\kappa\lambda_0}{2\sqrt{P}} \right\} \quad (27c)$$

The variance λ^{rs} , is determined as $\lambda^{rs} = \alpha^{-1}(\lambda_s + p)$ with

$$p = \lim_{n \uparrow \infty} \frac{1}{n} \|\mathbf{x}\|^2 = \mathbb{E}|x|^2 = \frac{\Xi}{(1 + \kappa\lambda)^2} + P e^{-\frac{\hat{\tau}^2}{\lambda^{rs}}}. \quad (28)$$

being the average transmit power of the precoder where

$$\Xi = (\lambda^{rs} + \tau^2) e^{-\frac{\tau^2}{\lambda^{rs}}} - (\lambda^{rs} + \tilde{\tau}^2) e^{-\frac{\tilde{\tau}^2}{\lambda^{rs}}}. \quad (29)$$

Moreover, $\kappa := \alpha^{-1}(1 + \chi)$ where χ satisfies

$$\chi = \frac{\kappa\Xi}{\lambda^{rs}(1 + \kappa\lambda)} + \frac{\kappa\hat{\tau}\sqrt{P}}{\lambda^{rs}} e^{-\frac{\hat{\tau}^2}{\lambda^{rs}}} + \kappa\sqrt{\frac{\pi P}{\lambda^{rs}}} Q\left(\sqrt{\frac{2}{\lambda^{rs}}}\hat{\tau}\right). \quad (30)$$

with $Q(\cdot)$ representing the standard Q-function. Considering (26), the decoupled precoded symbol is obtained from s^{rs} by a two steps hard thresholding. In the first step, s^{rs} is compared to $\tilde{\tau}$, in order to be constrained w.r.t. the peak power P . The second step, then, imposes the TAS constraint on the precoded symbol using the thresholds τ and $\hat{\tau}$. As a result, τ and $\hat{\tau}$

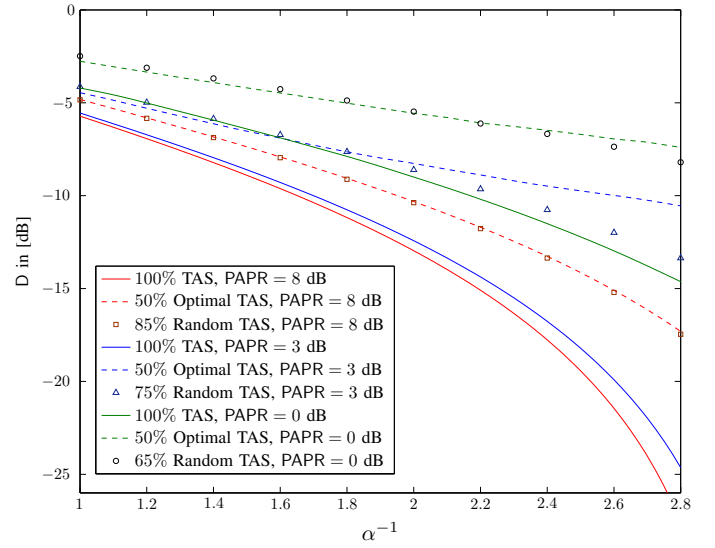


Fig. 2: Asymptotic distortion versus the inverse load factor for various constraints on the PAPR and η considering $p = 0.5$ and $\lambda_s = 1$. For PAPR = 8 dB, the precoder performs approximately same as the case with no peak power constraint, and thus, the gain obtained by the penalty function (19) is same as Fig 1. The gain, however, reduces for smaller PAPRs.

depend on the control factor λ_0 . By setting $\lambda_0 = 0$, we have $\tau = 0$ and $\hat{\tau} = \tilde{\tau}$, and thus, the precoder reduces to the PAPR limited precoder studied in [6]. To investigate the TAS and PAPR constraints imposed on the precoder, we further determine the asymptotic fraction of the active antennas, as well as the transmit signal's PAPR. Using Proposition 1, the asymptotic fraction of active antennas is given by

$$\eta = \lim_{n \uparrow \infty} \frac{1}{n} \|\mathbf{x}\|_0 = \mathbb{E} \mathbf{1}\{x \neq 0\} = e^{-\frac{\tau^2}{\lambda^{rs}}} + e^{-\frac{\tilde{\tau}^2}{\lambda^{rs}}} - e^{-\frac{\hat{\tau}^2}{\lambda^{rs}}}. \quad (31)$$

Moreover, considering the average transmit power p in (28), the asymptotic PAPR of the precoder is $\text{PAPR} = p^{-1}P$. Consequently, for given constraints on η and PAPR, the control factors λ and λ_0 and the scalar χ are found through the fixed point equations (28), (30) and (31), and the asymptotic distortion is determined as in (24).

In Fig. 2, the asymptotic distortion is given as a function of the inverse load factor for various constraints on the PAPR and number of active antennas considering $p = 0.5$ and $\lambda_s = 1$. For sake of comparison, we have also plotted the curves for PAPR limited precoders with random TAS fitted numerically to the curves of PAPR limited precoders with TAS constraint. As the figure depicts, at higher PAPRs, e.g., PAPR = 8 dB, the precoder outperforms random TAS with an approximately same reduction in the fraction of active antennas as for the case considered in Section IV-A (around $0.35n$). The result was also reported in [6] where the authors showed that the performance of PAPR limited precoders converges to the case with no peak power constraint in relatively small PAPRs. As the PAPR decreases to 0 dB, the reduction in the fraction of active antennas decreases as well. For example, as Fig. 2 illustrates, considering PAPR = 3 dB, the reduction is around

0.25n for load factors near to 1 while for the constant envelope case, i.e., PAPR = 0 dB, it reduces to 0.15n.

V. CONCLUSION

A general nonlinear LSE precoding scheme for the downlink of massive MIMO channels has been considered. The scheme addresses several hardware limitations on the transmitter including limited PAPR and number of active transmit antennas. Using the replica method from statistical mechanics, we have investigated the large-system performance of the precoder under the RS assumption. The numerical investigations have shown that for a given distortion at the receiver side, the proposed precoder needs 35% fewer active transmit antennas compared to the random TAS. An underway extension of this work is to consider Replica Symmetry Breaking (RSB) ansätze, in order to determine more accurate predictions of the performance in the regimes that RS fails.

APPENDIX

SKETCH OF THE PROOF

In this section, we explain the strategy for deriving Proposition 1. The proof is based on the replica method developed in statistical mechanics. The detailed derivations are omitted here and left for the extended version of the manuscript. To start with, consider the function

$$\mathcal{E}(\mathbf{v}|\mathbf{s}, \mathbf{H}) = \|\mathbf{H}\mathbf{v} - \mathbf{s}\|^2 + u(\mathbf{v}), \quad (32)$$

being referred to as the ‘‘Hamiltonian’’. We define the partition function $\mathcal{Z}(\beta, h)$ to be

$$\mathcal{Z}(\beta, h) = \sum_{\mathbf{v}} e^{-\beta\mathcal{E}(\mathbf{v}|\mathbf{s}, \mathbf{H}) + hnM_f^W(\mathbf{v}; n)}. \quad (33)$$

A. Evaluation of the Asymptotic Marginal

Using the standard large deviation argument, it is shown that the asymptotic marginal of $f(\mathbf{x})$ reads

$$M_f^W(\mathbf{x}) = \lim_{n \uparrow \infty} \lim_{\beta \uparrow \infty} \frac{\partial}{\partial h} \mathcal{F}(\beta, h)|_{h=0}, \quad (34)$$

where we have defined the function $\mathcal{F}(\cdot)$ to be

$$\mathcal{F}(\beta, h) := \frac{1}{n} \mathbb{E} \log \mathcal{Z}(\beta, h). \quad (35)$$

Therefore, the evaluation of the asymptotic marginal reduces to determination of the function $\mathcal{F}(\cdot)$. We further show that the asymptotic distortion is directly determined from $\mathcal{F}(\cdot)$.

B. Evaluation of the Asymptotic Distortion

Considering the Hamiltonian in (32), it can be shown that the asymptotic distortion satisfies

$$\alpha D + M_u^T(\mathbf{x}) = \tilde{\mathcal{E}} \quad (36)$$

where $M_u^T(\mathbf{x})$ denotes the asymptotic marginal of $u(\mathbf{x})$ over $\mathbb{T}(n) := [1 : n]$, and $\tilde{\mathcal{E}}$ is the asymptotic average energy of the Hamiltonian¹ defined as

$$\tilde{\mathcal{E}} = \lim_{n \uparrow \infty} \frac{1}{n} \mathbb{E} \mathcal{E}(\mathbf{x}|\mathbf{s}, \mathbf{H}). \quad (37)$$

¹In the context of statistical mechanics, $\tilde{\mathcal{E}}$ is the average energy of the spin glass defined by the Hamiltonian (32) in the thermodynamic limit.

Using (34), $M_u^T(\mathbf{x})$ is determined in terms of $\mathcal{F}(\cdot)$. Moreover,

$$\tilde{\mathcal{E}} = - \lim_{n \uparrow \infty} \lim_{\beta \uparrow \infty} \frac{\partial}{\partial \beta} \mathcal{F}(\beta, h)|_{h=0}. \quad (38)$$

Therefore, the asymptotic distortion D can be evaluated from $\mathcal{F}(\cdot)$ considering the equality in (36).

C. Determining $\mathcal{F}(\cdot)$

Considering the discussions in Sections A and B, the large-system analysis of the precoder reduces to determining the function $\mathcal{F}(\cdot)$. We do this task by employing the replica method which has been initially developed in statistical mechanics for analysis of spin glasses [17] and later employed in information theory to investigate the asymptotics of different problems; see [12]–[14], [18] and the references therein.

To determine $\mathcal{F}(\cdot)$, one needs to overcome the hard task of taking expectation of a logarithmic function. The task becomes analytically non-traceable when the argument of the logarithm is sum of exponential functions. Alternatively, one can employ the Riesz equality which states that for a random variable x

$$\mathbb{E} \log x = \lim_{m \downarrow 0} \frac{1}{m} \log \mathbb{E} x^m, \quad (39)$$

and bypasses the logarithmic expectation by writing $\mathcal{F}(\cdot)$ as

$$\mathcal{F}(\beta, h) = \frac{1}{n} \lim_{m \downarrow 0} \frac{1}{m} \log \mathbb{E} [\mathcal{Z}(\beta, h)]^m. \quad (40)$$

D. Replica Method

The computation of (40) is still non-trivial, since the right hand side (r.h.s.) of (40) needs to be determined for real values of m (or at least, for some m in a right neighborhood of 0). Replica method determines (40) by considering the conjecture of the replica continuity. The replica continuity indicates that the analytic continuation of the non-negative integer moment function, i.e., $\mathbb{E} [\mathcal{Z}(\beta, h)]^m$ for $m \in \mathbb{Z}^+$, onto the set of non-negative real numbers equals to the non-negative real moment function, i.e., $\mathbb{E} [\mathcal{Z}(\beta, h)]^m$ for $m \in \mathbb{R}_0^+$. More intuitively, it suggests us to determine the moment function as a function in $m \in \mathbb{Z}^+$, and then, assume that the function is of the same form for $m \in \mathbb{R}_0^+$. The rigorous justification of the replica continuity has not been yet precisely addressed; however, the analytic results from the theory of spin glasses confirm the validity of the conjecture for several cases. Following the replica continuity, the moment function $M(m) := \mathbb{E} [\mathcal{Z}(\beta, h)]^m$ reads

$$M(m) := \mathbb{E} \sum_{\{\mathbf{v}_a\}} \prod_{a=1}^m e^{-\beta\mathcal{E}(\mathbf{v}_a|\mathbf{s}, \mathbf{H}) + hnM_f^W(\mathbf{v}_a; n)} \quad (41a)$$

$$= \sum_{\{\mathbf{v}_a\}} \left[\mathbb{E} e^{-\beta \sum_{a=1}^m \mathcal{E}(\mathbf{v}_a|\mathbf{s}, \mathbf{H})} \right] e^{hn \sum_{a=1}^m M_f^W(\mathbf{v}_a; n)} \quad (41b)$$

where $\{\mathbf{v}_a\} := \{\mathbf{v}_1, \dots, \mathbf{v}_m\}$. Taking the expectation w.r.t. \mathbf{s} , the moment function reduces to

$$M(m) = \sum_{\{\mathbf{v}_a\}} \mathbb{E}_{\mathbf{J}} e^{-\beta \sum_{a,b=1}^m \mathbf{v}_a^H \mathbf{J} \mathbf{v}_b \xi_{ab} - n\Theta\{\mathbf{v}_a\}} \quad (42)$$

where $\xi_{ab} := \delta(a - b) - \lambda_s \beta (1 + \lambda_s \beta m)^{-1}$, \mathbf{J} denotes the Gramian of \mathbf{H} , i.e. $\mathbf{J} := \mathbf{H}^H \mathbf{H}$, and

$$\Theta\{\mathbf{v}_a\} := \frac{1}{n} \sum_{a=1}^m [\beta u(\mathbf{v}_a) - hn M_f^W(\mathbf{v}_a; n)] + \frac{1}{n} \Delta_m \quad (43)$$

with $\Delta_m := k \log(1 + \lambda_s \beta m)$. In order to take the expectation w.r.t. \mathbf{J} , we invoke the result reported in [19] for spherical integrals, where a closed form formula has been given under a set of assumptions. At this point, let us define \mathbf{Q}_m to be an $m \times m$ matrix with entries

$$[\mathbf{Q}_m]_{ab} = \frac{1}{n} \mathbf{v}_a^H \mathbf{v}_b. \quad (44)$$

Then, after taking the expectation w.r.t. \mathbf{J} , (42) reduces to

$$\mathbf{M}(m) = \sum_{\{\mathbf{v}_a\}} e^{-n\mathcal{G}(\mathbf{T}\mathbf{Q}_m) - n\Theta\{\mathbf{v}_a\}} \quad (45)$$

where $\mathbf{T} := \mathbf{I}_m - \lambda_s \beta (1 + \lambda_s \beta m)^{-1} \mathbf{1}_m$, and $\mathcal{G}(\cdot)$ reads

$$\mathcal{G}(\mathbf{M}) = \sum_{\ell=1}^m \int_0^{\beta \lambda_\ell} \mathbf{R}_D(-\omega) d\omega \quad (46)$$

for some matrix $\mathbf{M}_{m \times m}$ with eigenvalues $\{\lambda_\ell\}$ for $\ell \in [1 : m]$. The function $\mathbf{R}_D(\cdot)$ in (46) denotes the R-transform of the asymptotic distribution p_D defined in Definition 3. The sum in (45) can be determined by dividing the set of vectors $\{\mathbf{v}_a\}$ into subshells regarding \mathbf{Q}_m . More precisely, define the subshell $\mathcal{S}(\mathbf{Q})$ as the set of vectors $\{\mathbf{v}_a\}$ in which the corresponding matrix \mathbf{Q}_m equals to \mathbf{Q} ; then, (45) can be written as

$$\mathbf{M}(m) = \int e^{-n\mathcal{G}(\mathbf{T}\mathbf{Q}) - n\mathcal{I}(\mathbf{Q})} d\mathbf{Q} \quad (47)$$

where $d\mathbf{Q} := \prod_{a,b=1}^m d\text{Re}\{[\mathbf{Q}]_{ab}\} d\text{Im}\{[\mathbf{Q}]_{ab}\}$, the integral is taken over $\mathbb{C}^{m \times m}$, and $e^{-n\mathcal{I}(\mathbf{Q})}$ indicates the density of $\mathcal{S}(\mathbf{Q})$ which is written as

$$e^{-n\mathcal{I}(\mathbf{Q})} = \sum_{\{\mathbf{v}_a\}} e^{-n\Theta\{\mathbf{v}_a\}} w(\mathbf{Q}; \{\mathbf{v}_a\}) \quad (48)$$

with the weight function $w(\mathbf{Q}; \{\mathbf{v}_a\})$ being

$$w(\mathbf{Q}; \{\mathbf{v}_a\}) = \prod_{a,b=1}^m \delta(\text{Re}\{n[\mathbf{Q}]_{ab} - \mathbf{v}_a^H \mathbf{v}_b\}) \times \delta(\text{Im}\{n[\mathbf{Q}]_{ab} - \mathbf{v}_a^H \mathbf{v}_b\}). \quad (49)$$

The weight function (49) is further calculated in an analytic form using the Laplace inverse transform of the impulse function $\delta(\cdot)$.

At this point, $\mathcal{F}(\cdot)$ is determined by substituting (47) in (40) and taking the limits. We assume that the limits w.r.t. n and m commute. This assumption is common in replica analyses and is intuitively concluded from the analytic continuity of the moment function being conjectured by the replica continuity. Consequently, n in (47) can be considered to grow large, and thus, by the saddle point method, one can conclude that

$$\mathbf{M}(m) \doteq K_n e^{-n[\mathcal{G}(\mathbf{T}\tilde{\mathbf{Q}}) + \mathcal{I}(\tilde{\mathbf{Q}})]} \quad (50)$$

where \doteq denotes the asymptotic logarithmic equivalence¹, K_n is a non-negative real sequence in n bounded for any n , and $\tilde{\mathbf{Q}}$ is the saddle point of the exponent function.

E. RS assumption

The next step is to determine the saddle point $\tilde{\mathbf{Q}}$, explicitly by searching over all possible $m \times m$ matrices consistent with (44). The task, however, is not feasible, due to the both complexity and analyticity issues. In fact, one may find the above task to be computationally complex. Moreover, some of the solutions for the saddle point may result in non-analytic moment functions which cannot be analytically continued to the real axis, and thus, are not of use. To address both the issues, we invoke the well-known trick from theory of spin glasses which suggests to restrict the search to a set of parameterized matrices. The known structures for these sets are conjectured from the physical intuition behind the replica analysis and are mainly RS or RSB. In RS, the replicas, i.e., $\{\mathbf{v}_a\}$, are assumed to behave symmetrically at the saddle point meaning that interactions between any two replicas \mathbf{v}_a and \mathbf{v}_b are the same. Therefore, due to (44), $\tilde{\mathbf{Q}}$ in this case is invariant under all permutations, meaning that $\mathbf{P}^{-1} \tilde{\mathbf{Q}} \mathbf{P} = \tilde{\mathbf{Q}}$ for all permutation matrices \mathbf{P} taken from the symmetric group on $[1 : m]$. This assumption leads to the following structure

$$\tilde{\mathbf{Q}} = \frac{\chi}{\beta} \mathbf{I}_m + p \mathbf{1}_m \quad (51)$$

for some non-negative real scalars χ and p . For various problems, the RS structure results in solutions which are consistent with the available rigorous bounds [12], [13], [18], [20]. There are, however, several examples in which the RS ansatz does not give valid solutions [6], [14], [21], [22]. For these cases, it is believed that the problem is caused by the assumed structure, i.e., RS, and therefore, more general structures are supposed to result in valid solutions. In [23], Parisi proposed the iterative method of RSB which extends RS to a sequence of more general structures. The authors in [6], [14], [21], employed Parisi's method to investigate the examples with invalid RS ansatz considering RSB ansätze. We believe that the examples in Sections IV-A and IV-B, at least for the range of system parameters which we consider, are investigated by the RS ansatz considerably accurate. Therefore, at this point we consider $\tilde{\mathbf{Q}}$ to be of the form (51), and leave the derivation of RSB ansätze as a future work. After some lines of derivations, the scalars χ and p at the saddle point are found as

$$p = \int |\arg \min_v \mathcal{E}_{rs}(v|s_0)|^2 Ds_0, \quad (52a)$$

$$\chi = \frac{1}{\varsigma} \int \text{Re} \left\{ \arg \min_v \mathcal{E}_{rs}(v|s_0) s_0^* \right\} Ds_0, \quad (52b)$$

where $\mathcal{E}_{rs}(\cdot|s_0) : \mathbb{X} \mapsto \mathbb{R}$ for a given $s_0 \in \mathbb{C}$ is defined as

$$\mathcal{E}_{rs}(v|s_0) := |v - \frac{\varsigma}{\mathbf{R}_D(-\chi)} s_0|^2 + \frac{u(v)}{\mathbf{R}_D(-\chi)}, \quad (53)$$

¹ $a_n \doteq b_n$ if $\lim_{n \uparrow \infty} |\frac{a_n}{b_n}| = 0$.

$D_{s_0} := \frac{1}{\pi} e^{-|s_0|^2} d\text{Re}\{s_0\} d\text{Im}\{s_0\}$, and ς is given by

$$\varsigma^2 = \frac{\partial}{\partial \chi} [(\lambda_s \chi - \mathfrak{p}) R_{\mathbf{D}}(-\chi)]. \quad (54)$$

The function $\mathcal{F}(\cdot)$ is then determined by substituting $\tilde{\mathbf{Q}}$ with χ and \mathfrak{p} given in (52a) and (52b). Considering the discussions in Sections A and B, the asymptotic marginal of $f(\mathbf{x})$ is calculated as

$$M_f^{\mathbf{W}}(\mathbf{x}) = \int f\left(\arg \min_v \mathcal{E}_{rs}(v|s_0)\right) D_{s_0}, \quad (55)$$

and the asymptotic distortion is determined by

$$D = \lambda_s + \alpha^{-1} \frac{\partial}{\partial \chi} [(\mathfrak{p} - \lambda_s \chi) \chi R_{\mathbf{D}}(-\chi)] \quad (56)$$

Defining the scalar $\lambda^s = \varsigma [R_{\mathbf{D}}(-\chi)]^{-1}$, Proposition 1 is finally concluded. Detailed derivations of this section are given in the extended version of the manuscript.

REFERENCES

- [1] T. L. Marzetta, "Noncooperative cellular wireless with unlimited numbers of base station antennas," *IEEE Trans. on Wireless Comm.*, vol. 9, no. 11, pp. 3590–3600, 2010.
- [2] T. S. Rappaport, S. Sun, R. Mayzus, H. Zhao, Y. Azar, K. Wang, G. N. Wong, J. K. Schulz, M. Samimi, and F. Gutierrez, "Millimeter wave mobile communications for 5G cellular: It will work!" *IEEE access*, vol. 1, pp. 335–349, 2013.
- [3] R. F. Fischer, C. Windpassinger, A. Lampe, and J. B. Huber, "Space-time transmission using Tomlinson-Harashima precoding," *ITG FACHBERICHT*, pp. 139–148, 2002.
- [4] C. B. Peel, B. M. Hochwald, and A. L. Swindlehurst, "A vector-perturbation technique for near-capacity multiantenna multiuser communication – Part I: channel inversion and regularization," *IEEE Trans. on Comm.*, vol. 53, no. 1, pp. 195–202, 2005.
- [5] S. K. Mohammed and E. G. Larsson, "Per-antenna constant envelope precoding for large multi-user MIMO systems," *IEEE Trans. on Comm.*, vol. 61, no. 3, pp. 1059–1071, 2013.
- [6] M. A. Sedaghat, A. Beryhi, and R. Müller, "A new class of nonlinear precoders for hardware efficient massive MIMO systems," *IEEE International Conference on Communications (ICC)*, 2017.
- [7] A. F. Molisch, M. Z. Win, Y.-S. Choi, and J. H. Winters, "Capacity of MIMO systems with antenna selection," *IEEE Trans. on Wireless Comm.*, vol. 4, no. 4, pp. 1759–1772, 2005.
- [8] M. Gharavi-Alkhansari and A. B. Gershman, "Fast antenna subset selection in MIMO systems," *IEEE Trans. on Signal Processing*, vol. 52, no. 2, pp. 339–347, 2004.
- [9] A. Gorokhov, D. A. Gore, and A. J. Paulraj, "Receive antenna selection for MIMO spatial multiplexing: theory and algorithms," *IEEE Trans. on Signal Processing*, vol. 51, no. 11, pp. 2796–2807, 2003.
- [10] H. Li, L. Song, and M. Debbah, "Energy efficiency of large-scale multiple antenna systems with transmit antenna selection," *IEEE Trans. on Comm.*, vol. 62, no. 2, pp. 638–647, 2014.
- [11] S. Asaad, A. Beryhi, R. R. Müller, and A. M. Rabiei, "Asymptotics of transmit antenna selection: Impact of multiple receive antennas," *IEEE International Conference on Communications (ICC)*, 2017.
- [12] D. Guo and S. Verdú, "Randomly spread CDMA: Asymptotics via statistical physics," *IEEE Trans. on Inf. Theory*, vol. 51, no. 6, pp. 1983–2010, 2005.
- [13] S. Rangan, A. Fletcher, and V. Goyal, "Asymptotic analysis of MAP estimation via the replica method and applications to compressed sensing," in *IEEE Trans. on Inf. Theory*, 2012, pp. 1902–1923.
- [14] A. Beryhi, R. Müller, and H. Schulz-Baldes, "RSB decoupling property of MAP estimators," *IEEE Information Theory Workshop (ITW)*, pp. 379–383, 2016.
- [15] N. I. Akhiezer, *The classical moment problem: and some related questions in analysis*. Oliver & Boyd, 1965, vol. 5.
- [16] R. R. Müller, G. Alfano, B. M. Zaidel, and R. de Miguel, "Applications of large random matrices in communications engineering," *arXiv preprint arXiv:1310.5479*, 2013.
- [17] S. F. Edwards and P. W. Anderson, "Theory of spin glasses," *Journal of Physics F: Metal Physics*, vol. 5, no. 5, p. 965, 1975.
- [18] T. Tanaka, "A statistical-mechanics approach to large-system analysis of CDMA multiuser detectors," *IEEE Trans. on Inf. Theory*, vol. 48, no. 11, pp. 2888–2910, 2002.
- [19] A. Guionnet, M. Mai *et al.*, "A fourier view on the R-transform and related asymptotics of spherical integrals," *Journal of functional analysis*, vol. 222, no. 2, pp. 435–490, 2005.
- [20] R. Müller, D. Guo, and A. L. Moustakas, "Vector precoding for wireless MIMO systems and its replica analysis," *IEEE Journal on Selected Areas in Comm.*, vol. 26, no. 3, pp. 530–540, 2008.
- [21] B. M. Zaidel, R. Müller, A. L. Moustakas, and R. de Miguel, "Vector precoding for Gaussian MIMO broadcast channels: Impact of replica symmetry breaking," *IEEE Trans. on Inf. Theory*, vol. 58, no. 3, pp. 1413–1440, 2012.
- [22] A. Beryhi, R. R. Müller, and H. Schulz-Baldes, "Statistical mechanics of MAP estimation: General replica ansatz," *arXiv preprint arXiv:1612.01980*, 2016.
- [23] G. Parisi, "A sequence of approximated solutions to the SK model for spin glasses," *Journal of Physics A: Mathematical and General*, vol. 13, no. 4, p. L115, 1980.